

ANALYSIS OF BACKWARD PROTON- ^3He AND ^4He ELASTIC SCATTERING AT INTERMEDIATE ENERGIES

BY H. LEŚNIAK AND L. LEŚNIAK

Institute of Nuclear Physics, Cracow*

(Received November 9, 1977)

Recent experimental data on the backward scattering of protons on ^3He and ^4He are analysed using the deuteron and triton exchange models. The absorption effects, which are included in the eikonal approximation, can change the cross section calculated in the plane wave Born approximation by one or two orders of magnitude. The theoretical predictions are compared with recent experimental data.

1. Introduction

New experimental data on the backward proton- ^4He [1] and proton- ^3He [2] elastic scattering have been recently obtained at Saclay. The ^4He data at 298, 438 and 648 MeV have been analysed in the framework of the triton exchange model [3]. It has been shown that the exchange amplitude is very sensitive to the high momentum components of the exchanged particle wave function. The absorption effects, which are due to the proton-proton or proton-triton interactions in addition to the triton exchange, influence very much the differential cross section changing its magnitude and the shape. In the present paper we analyse the ^4He data at 6.0 GeV/c α -particle momentum which corresponds to 840 MeV incoming proton kinetic energy and the p - ^3He data at 415, 600 and 800 MeV. For the description of the ^3He data we use the deuteron exchange model including the absorption effects. Since this model is very similar to the triton exchange model described in Ref. [3], in Section 2 we repeat only the main formulae for the p - ^3He exchange amplitude. Section 3 contains the numerical results for the p - ^3He differential cross sections and Section 4 gives the results for the proton scattering on the ^4He target. Conclusions are given in Section 5.

2. Derivation of the exchange amplitude for the p - ^3He scattering

The exchange process of the elastic p - ^3He scattering is schematically illustrated in Fig. 1. By d we denote the proton-neutron pair which forms the initial ^3He nucleus together with the proton p_1 and remains in the final ^3He nucleus with the incoming proton p .

* Address: Instytut Fizyki Jądrowej, Radzikowskiego 152, 31-342 Kraków, Poland.

This pair we shall call deuteron although in general it may have the spin-isospin quantum numbers different from the deuteron ones. The diagram corresponding to this mechanism is shown in Fig. 2a. This is so-called plane wave Born approximation of the exchange amplitude which in the general case contains the initial and final state interactions repre-

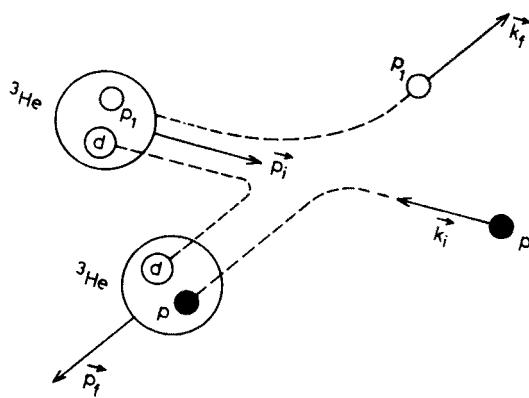


Fig. 1. Exchange process of elastic p-³He scattering

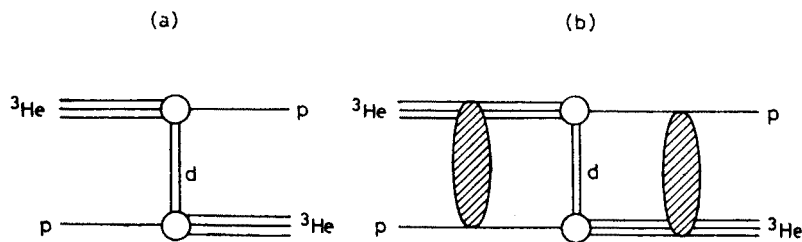


Fig. 2. a) Deuteron exchange diagram, b) deuteron exchange diagram including absorption

sented as the shaded area in Fig. 2b. The exchange amplitude is given by the formula [4]:

$$\mathcal{T}^{ex} = \langle \phi^- | V_{p_1 d} | \psi^+ \rangle, \tag{2.1}$$

where $V_{p_1 d}$ is the proton p_1 -d interaction, ψ^+ is the wave function describing the entire scattering process

$$\psi^+ = \chi_i + \frac{1}{E + i\eta - H} V \chi_i \tag{2.2}$$

and ϕ^- describes the scattering of two protons p and p₁,

$$\phi^- = \chi_f + \frac{1}{E - i\eta - (H - V_{p_1 d})} V_{pp_1} \chi_f; \quad \eta \rightarrow +0. \tag{2.3}$$

In Eqs (2.2) and (2.3) H is the total Hamiltonian, E is the total energy, V is the initial channel interaction

$$V = V_{pp_1} + V_{pd} \quad (2.4)$$

and V_{pp_1} is the interaction of the protons p and p_1 . The initial wave function χ_i is

$$\chi_i = (2\pi)^{-3} e^{i\vec{k}_i \cdot \vec{r}_p} u_{v_i}(s_p) e^{i\vec{P}_i \cdot \vec{R}_i} \varphi_{\varepsilon_i}^h(\vec{r}_1, \vec{r}_2, \vec{r}_3), \quad (2.5)$$

where \vec{k}_i , \vec{r}_p and s_p are the momentum, space and spin coordinates of the initial proton while $u_{v_i}(s_p)$ is its spin wave function with spin projection v_i ; \vec{P}_i , \vec{R}_i and ε_i are the ${}^3\text{He}$ -nucleus momentum, position coordinates and spin projection. The internal ${}^3\text{He}$ wave function $\varphi_{\varepsilon_i}^h$ depends only on two coordinate vectors because the following condition is satisfied

$$\vec{R}_i = \frac{1}{3} (\vec{r}_1 + \vec{r}_2 + \vec{r}_3), \quad (2.6)$$

where \vec{r}_1 and \vec{r}_2 are the coordinates of two protons and \vec{r}_3 is the neutron coordinate. The final wave function is given by the formula:

$$\chi_f = (2\pi)^{-3} e^{i\vec{k}_f \cdot \vec{r}_f} u_{v_f}(s_f) e^{i\vec{P}_f \cdot \vec{R}_f} \varphi_{\varepsilon_f}^h(\vec{r}_p, \vec{r}_2, \vec{r}_3), \quad (2.7)$$

where \vec{k}_f is the final proton momentum, v_f — its spin projection and \vec{P}_f and ε_f — the final ${}^3\text{He}$ momentum and spin projection. The coordinate \vec{R}_f is equal to

$$\vec{R}_f = \frac{1}{3} (\vec{r}_p + \vec{r}_2 + \vec{r}_3). \quad (2.8)$$

The wave functions $\varphi_{\varepsilon_i}^h$ and $\varphi_{\varepsilon_f}^h$ are translationally invariant. The normalization of the amplitude is such that the contribution of the exchange amplitude to the differential cross section in the c. m. system for an unpolarized proton beam and unpolarized ${}^3\text{He}$ target is

$$\frac{d\sigma}{d\Omega} = (2\pi)^4 \left(\frac{E_p E_h}{E_p + E_h} \right)^2 \frac{1}{4} \sum_{v_i \varepsilon_i v_f \varepsilon_f} |2T_{v_i \varepsilon_i v_f \varepsilon_f}|^2, \quad (2.9)$$

where E_p and E_h are the proton and ${}^3\text{He}$ -particle c. m. energies and the amplitude $T_{v_i \varepsilon_i v_f \varepsilon_f}$ multiplied by the Dirac delta function $\delta(\vec{k}_i + \vec{p}_i - \vec{k}_f - \vec{p}_f)$ gives the amplitude \mathcal{T}^{ex} (Eq. (2.1)). The factor 2 before T in Eq. (2.9) means that there are two possible exchanges of the incident proton with two protons of ${}^3\text{He}$ nucleus.

Now we shall make a set of assumptions needed in the calculation of the exchange amplitude. The wave functions ϕ^- and ψ^+ are written in the eikonal approximation:

$$\phi^{-*} = \chi_f^* \exp \left[-\frac{i}{v} \int_{z_p}^{\infty} V_{pp_1}(\vec{b}_p + \hat{k}_z, \vec{r}_1) dz \right], \quad (2.10)$$

$$\psi^+ = \exp \left[-\frac{i}{v} \int_{-\infty}^{z_p} V(\vec{b}_p + \hat{k}_z, \vec{r}_1, \vec{r}_2, \vec{r}_3) dz \right] \chi_i, \quad (2.11)$$

where the z -axis is chosen along a vector $\hat{k} = (\vec{k}_i - \vec{k}_f) / |\vec{k}_i - \vec{k}_f|$, so b_p is the perpendicular component of the vector \vec{r}_p , $\hat{k}z$ — its longitudinal component and v is the relative p - ^3He velocity in the c.m. system. Next we introduce some relative vectors (see Fig. 3):

$$y_1 = \vec{r}_3 - \vec{r}_2, \quad (2.12)$$

$$\vec{y} = \vec{r}_1 - \vec{r}_d, \quad (2.13)$$

$$\vec{\varrho} = \vec{r}_p - \vec{r}_d, \quad (2.14)$$

where

$$r_d = \frac{1}{2} (\vec{r}_2 + \vec{r}_3). \quad (2.15)$$

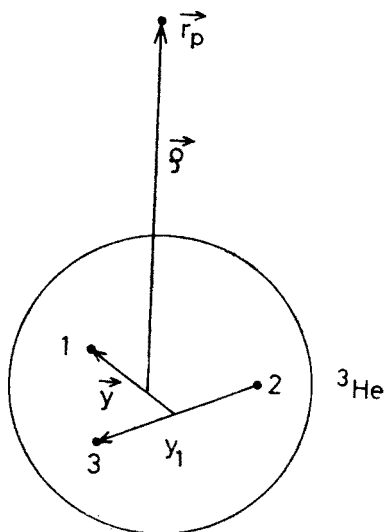


Fig. 3. Relative coordinates in ^3He

We assume that the interactions V_{pp_1} , V_{p_1d} and V_{pd} are the functions which depend only on the relative coordinates $\vec{\varrho} - \vec{y}$, \vec{y} and $\vec{\varrho}$ and are independent on spins. Therefore it is very convenient to take the ^3He wave function in the factorized form

$$\varphi_{e_1}^h(\vec{r}_1, \vec{r}_2, \vec{r}_3) = \chi(y) \cdot \lambda_{e_1}(\vec{y}_1), \quad (2.16)$$

where the function $\chi(y)$ describes the s -state relative motion of the n - p pair with respect to the proton p_1 and $\lambda_{e_1}(\vec{y}_1)$ describes the internal motion of the n - p pair and contains the spin coupling of the three nucleons. The final ^3He wave function is

$$\varphi_{e_1}^h(\vec{r}_p, \vec{r}_2, \vec{r}_3) = \chi(\varrho) \lambda_{e_1}(\vec{y}_1). \quad (2.17)$$

There is a large probability that the p - n pair forms the deuteron which has isospin 0 and spin 1. As in Ref. [5] we assume that this probability is unity, so for λ_{e_1} we adopt the following spin coupling:

$$\lambda_{e_1} = \sum_{\nu\sigma} \langle \frac{1}{2} \nu 1 \sigma | \frac{1}{2} e_1 \rangle \psi_{\sigma}^d(\vec{y}_1) u_{\nu}(s_1), \quad (2.18)$$

where $\psi_\sigma^d(\vec{y}_1)$ denotes the deuteron wave function and $u_v(s_1)$ is the proton p_1 spinor, σ and v are the deuteron and proton spin projections. For λ_{e_f} we can write the expression similar to Eq. (2.18) replacing s_1 by s_p and ε_i by ε_f .

The relative motion wave function $\chi(y)$ satisfies the Schrödinger equation

$$\left[-\frac{\nabla_y^2}{2\mu} + V_{p,d}(y) \right] \chi(y) = \varepsilon_s \chi(y), \quad (2.19)$$

where μ is the proton-deuteron reduced mass and

$$\varepsilon_s = \varepsilon_h - \varepsilon_d = -5.49 \text{ MeV} \quad (2.20)$$

is the proton separation energy in ^3He (ε_h and ε_d are ^3He and deuteron binding energies).

Using the above assumption we get the amplitude

$$T_{v_i \varepsilon_i v_f \varepsilon_f} = t_{v_i \varepsilon_i v_f \varepsilon_f} T_{ex} \quad (2.21)$$

with the numerical factor

$$t_{v_i \varepsilon_i v_f \varepsilon_f} = u_{v_f}^\dagger(s_1) \int d^3 y_1 \lambda_{e_f}^*(\vec{y}_1) \lambda_{e_i}(\vec{y}_1) u_{v_i}(s_p) \quad (2.22)$$

and the amplitude

$$T_{ex} = (2\pi)^{-3} \int d^3 y d^3 \varrho \exp(i\vec{Q}_p \vec{\varrho} + i\vec{Q}_y \vec{y}) \chi^*(\varrho) \left(\varepsilon_s + \frac{\nabla_y^2}{2\mu} \right) \chi(y) f(\vec{\varrho}, \vec{y}). \quad (2.23)$$

In Eq. (2.23) the two vectors are introduced

$$\vec{Q}_p = \vec{k}_i - \frac{1}{3} \vec{p}_f, \quad (2.24)$$

$$\vec{Q}_y = \frac{1}{3} \vec{p}_i - \vec{k}_f \quad (2.25)$$

and $f(\vec{\varrho}, \vec{y})$ is the absorption factor

$$f(\vec{\varrho}, \vec{y}) = \exp \left[-\frac{i}{v} \int_{-\infty}^{\infty} V_{pp_1}(\vec{\varrho}_\perp - \vec{y}_\perp, z) dz - \frac{i}{v} \int_{-\infty}^{\varrho_z} V_{pd}(\vec{\varrho}_\perp, z) dz \right]. \quad (2.26)$$

Here $\vec{\varrho}_\perp$ and \vec{y}_\perp are the perpendicular components of vectors $\vec{\varrho}$ and \vec{y} and ϱ_z is the parallel component of $\vec{\varrho}$ with respect to the z -axis taken along $\vec{k}_i - \vec{k}_f$.

The cross section (2.9) corresponding to the amplitude (2.21) is

$$\frac{d\sigma}{d\Omega} = \frac{4}{3} (2\pi)^4 \left(\frac{E_p E_h}{E_p + E_h} \right)^2 |T_{ex}|^2, \quad (2.27)$$

where the factor $4/3$ comes from the summation over the spin projections

$$\frac{1}{4} \sum_{v_i \varepsilon_i v_f \varepsilon_f} |2t_{v_i \varepsilon_i v_f \varepsilon_f}|^2 = \frac{4}{3}. \quad (2.28)$$

In the calculation of Eq. (2.28) we used the orthonormality relations for the proton spinors and the deuteron wave functions. The internal deuteron structure may be arbitrary in this calculation.

When the absorption factor is equal to 1, we obtain the Born amplitude in the c.m. system

$$T_{\text{ex}}^{\text{B}}(Q) = (2\pi)^{-3} \left(\varepsilon_s - \frac{Q^2}{2\mu} \right) H^2(Q), \quad (2.29)$$

where $H(Q)$ is the Fourier transform of $\chi(r)$

$$H(Q) = \int d^3r e^{i\vec{Q}\cdot\vec{r}} \chi(r) \quad (2.30)$$

and we have assumed that $\chi(r)$ is the real function. The parametrization of the function $\chi(r)$ is the following (Ref. [5]):

$$\chi(r) = N \frac{1}{r} \exp(-\alpha r) [1 - \exp(-\beta r)]^n. \quad (2.31)$$

In this equation N is the normalization constant,

$$\alpha = \sqrt{-2\mu\varepsilon_s} = 0.420 \text{ fm}^{-1}$$

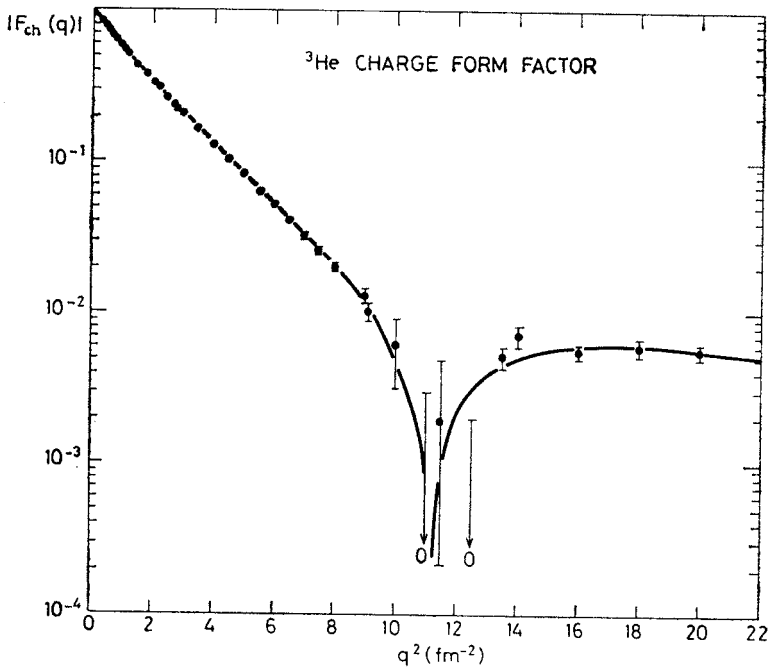


Fig. 4. The ${}^3\text{He}$ charge form factor. Data are from Ref. [6]

and β and n are real parameters fitting the electromagnetic ${}^3\text{He}$ form factor which is proportional to the body form factor:

$$F(q) = \int d^3r e^{i\vec{q}\cdot\vec{r}} |\chi(r)|^2. \quad (2.32)$$

In Fig. 4 we see that a good fit to experiment [6] is obtained for $\beta = 1.80 \text{ fm}^{-1}$ and $n = 4$. In this fit the proton and neutron electromagnetic form factors are taken from Ref. [7]. In Fig. 5 the function $|H(k)|$ is plotted. It has a zero at $k^2 \approx 4 \text{ fm}^{-2}$.

In order to specify the form of the absorption factor (2.26) we express the part of f containing the proton-proton interaction by the profile function

$$\gamma_{pp}(\vec{q}_\perp - \vec{y}_\perp) = 1 - \exp \left[-\frac{i}{v} \int_{-\infty}^{\infty} V_{pp1}(\vec{q}_\perp - \vec{y}_\perp, z) dz \right], \quad (2.33)$$

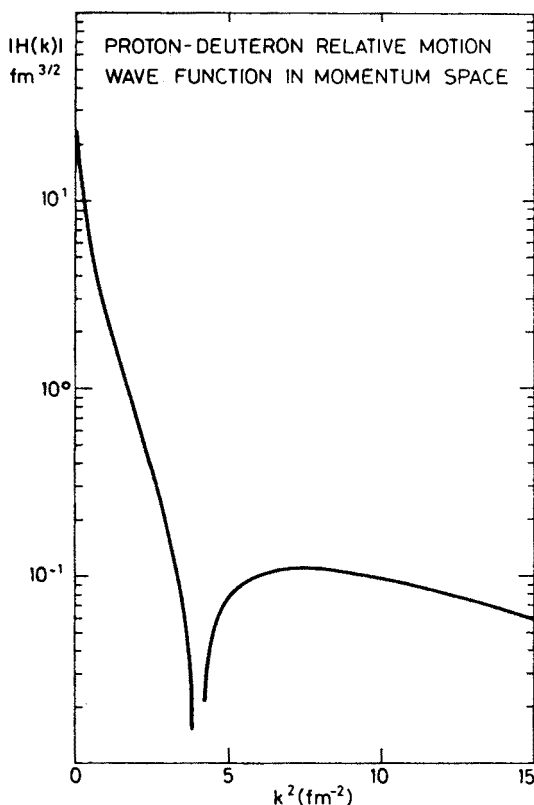


Fig. 5. Proton-deuteron relative motion wave function in momentum representation (Eqs (2.30)–(2.31))

which is related to the proton-proton elastic scattering amplitude

$$f_{pp}(q) = \frac{ik}{2\pi} \int d^2b e^{i\vec{q}\vec{b}} \gamma_{pp}(b) \quad (2.34)$$

parametrized as the Gaussian function of momentum transfer q

$$f_{pp}(q) = \frac{(i + \alpha_p) \sigma_p k}{4\pi} e^{-\frac{\alpha_p}{2} q^2}, \quad (2.35)$$

The parameters of this *effective* amplitude are: the total proton-proton cross section σ_p , the ratio α_p of the real to the imaginary part of the forward scattering amplitude and the slope parameter α_p .

The proton-deuteron interaction is parametrized in the following form

$$\frac{1}{v} V_{pd}(r) = \text{Re } \varepsilon(i + \alpha_d)2 \sqrt{\frac{B}{\pi}} e^{-Br^2} \tag{2.36}$$

where $\text{Re } \varepsilon$, α_d and β are real constants to be fitted from experiment.

The above equation completes the set of the functions needed in the calculation of the exchange amplitude (2.23).

3. Numerical results for $p\text{-}^3\text{He}$ scattering

The differential cross sections have been calculated numerically using Eqs (2.23) and (2.27). Some integrations have been done analytically as described in the appendix of Ref. [3]. The results are shown in Fig. 6 and the parameters used are given in Table I.

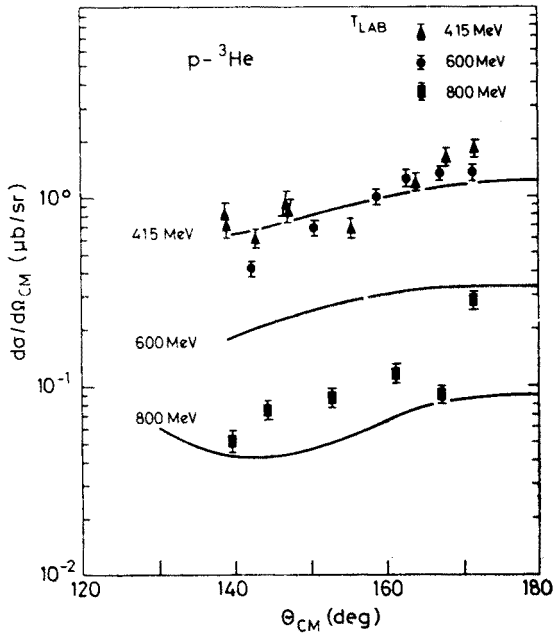


Fig. 6. Proton- ^3He elastic scattering at 415, 600 and 800 MeV. Data are from Ref. [2]. Parameters are given in Table I

A rather good agreement with experimental data at 415 MeV is obtained while at 600 MeV and 800 MeV the theoretical curves lie too low. The remarkable fact is that the 415 and 600 MeV angular distributions are experimentally almost identical. This is impossible to achieve in the Born approximation but the absorption effects are so strong that it

TABLE I

Parameters used in the calculations of the p-³He cross sections

Energy MeV	σ_p mb	α_p	a_p GeV ⁻²	Re ε	α_d	B fm ⁻²
325	24.0	0.70	0.4	-0.23	0.35	0.45
415	26.5	0.61	0.4	-0.25	0.30	0.45
600	37.0	0.48	3.0	-0.30	0.15	0.45
800	47.5	0.27	5.0	-0.34	-0.09	0.45

can change substantially the Born cross sections as it is shown in Fig. 7. Although the angular distributions in the Born approximation are quite different, the absorption corrections make the two cross sections very close at 325 and 415 MeV. Let us notice that at these energies the absorption corrections are *positive* while at higher energies like at 600 or 800

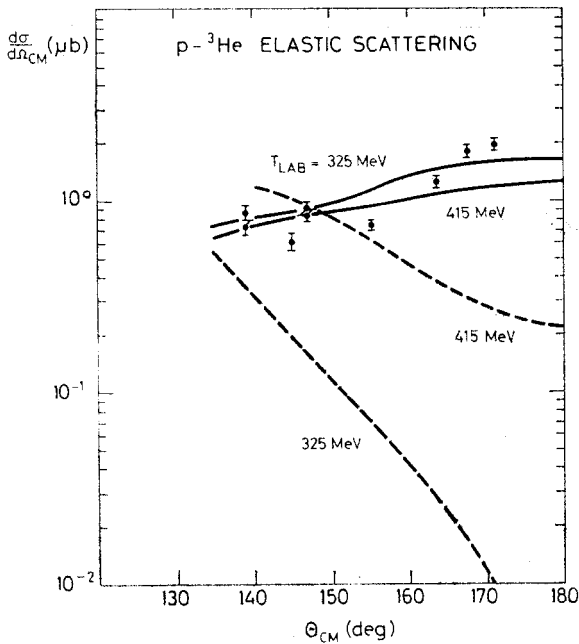


Fig. 7. Comparison of the p-³He differential cross sections at 325 and 415 MeV. The dashed lines are calculated in the Born approximation, the solid curves present the absorption effects. The experimental points are from Ref. [2] at 415 MeV

800 MeV they are *negative* (Figs 8, 9). At 600 MeV the cross section in the Born approximation is larger than the experimental one but when the absorption effects are included the theoretical cross section is considerably smaller than the the experimental one. In the same figure the dependence on the ratio α_p is shown and the upper curve corresponds

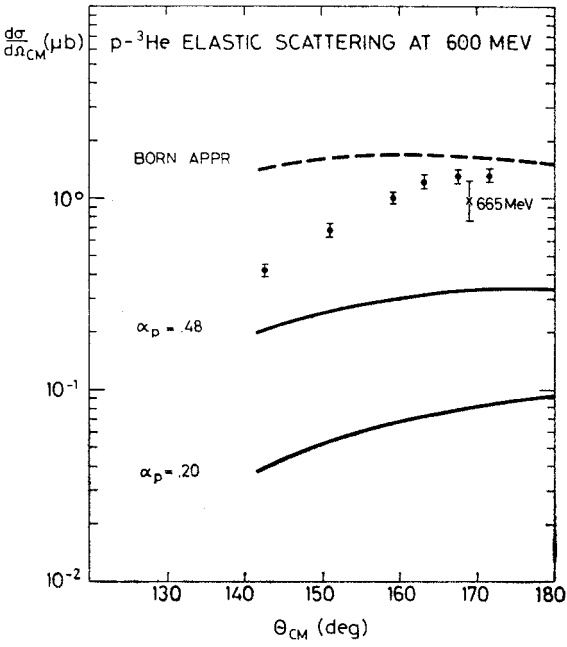


Fig. 8. Proton- ^3He elastic scattering at 600 MeV. Data are from Ref. [2], the crossed point is from Ref. [20]. The theoretical curves are calculated for two different values of ratio α_p of the p-p forward amplitude

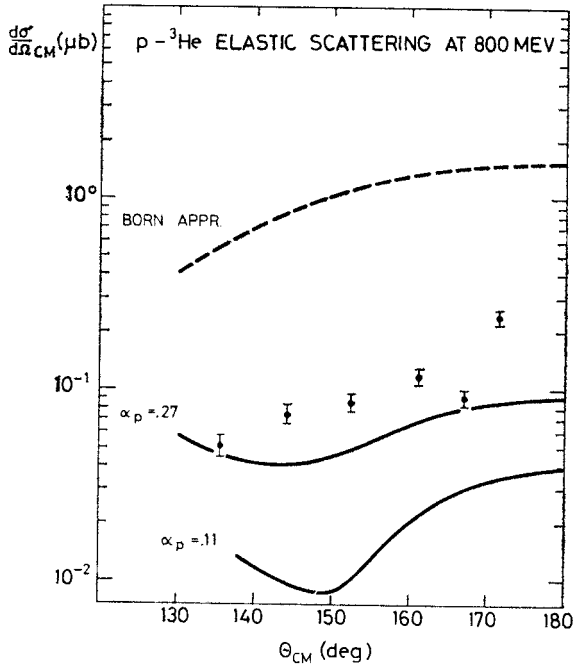


Fig. 9. Proton- ^3He elastic scattering at 800 MeV. Data are from Ref. [2]. The theoretical curves correspond to two different values of parameter α_p

rather to the maximum value of α_p compatible with the experimental pp data [8, 9] or the dispersion relations calculations [10, 11]. The total cross section σ_p and the slope a_p are also taken from experiments (Refs [12–14]). The parameters of the pd interaction have been obtained by a comparison of the total pd cross sections and the small angle differential cross sections with the experimental values of Refs [12, 13, 15–19]. The theoretical pd amplitude has been calculated in the eikonal approximation. At 800 MeV the cross section in the Born approximation is larger than the experimental one by a factor ten but when the absorption effects are added it is even smaller than the experimental one. We observe that the role of absorption increases with increasing energy and that some disagreement in the absolute magnitude of the angular distributions remains at 600 MeV. The general shape of the differential cross sections is, however, reproduced.

One may list many effects which can contribute to the p - ^3He scattering amplitude in addition to the deuteron exchange. The first possibility is that the exchanged n - p pair is not in 100% in the $S = 1$, isospin 0 state. In fact the ^3He structure is more complicated and the full ^3He wave function contains S , S' and D components [21]. The orbital parts of these wave functions are not well known especially at high momentum transfers and many calculations using the “realistic” ^3He wave functions underestimate the ^3He charge form factor at the secondary maximum [22]. Therefore we have used the simple form (2.31) which has the correct asymptotic behaviour at large p - d distances and fits the electromagnetic ^3He form factor. Let us remark here that in order to calculate the contributions to the cross section coming from the other possible states of the exchanged n - p pair, we have to use the different spin factors and different absorption factors (Eq. (2.26)). For example, if we neglect the absorption effects and use the completely antisymmetrized wave function in the spin and isospin coordinates of three ^3He nucleons (being in the relative S -state orbital motion), then the factor $\frac{4}{3}$ in Eq. (2.28) becomes unity. In this case the probability of the n - p pair in the 3S_1 , isospin 0 state is equal to $\frac{1}{2}$ and the same is the probability of the 1S_0 , isospin 1 state. The interaction of the n - p pair in the 1S_0 state (which is not a bound state) with the proton is, however, more difficult to calculate than the deuteron-proton interaction which experimentally is much better known.

The second possibility of explaining the behaviour of the p - ^3He cross section in the 400–800 MeV energy range is an exchange of a pion in addition to the two-nucleon pair. This possibility has been mentioned in Ref. [2] but already in Ref. [23] the cross section at 180° has been calculated using the one pion exchange model and the cross section for the $pd \rightarrow \pi t$ reaction. Unfortunately the calculated cross section has been considerably smaller than the experimental result and paradoxically deuteron-exchange contribution has been indicated as a possible source of this discrepancy. It seems to us, however, that some assumptions of Ref. [23] should be reexamined once again before the final conclusion about an inapplicability of the two-nucleon plus one pion exchange model can be drawn.

We would like to mention briefly some other contributions to the calculated cross section. It is known that the nucleon-nucleon amplitudes depend on spins and vary much with energy. Since the ^3He nucleus has spin $\frac{1}{2}$ we may expect that the spin amplitudes may be important. In the present paper we use only the *effective* spin-independent pp or

pd interactions in order to simplify the calculations. Moreover the direct amplitude which dominates the forward scattering has been neglected. It is now extremely difficult to calculate it accurately because we do not know the high momentum components of the ${}^3\text{He}$ wave function which are more important for the direct amplitude than for the exchange one. One may expect that in this case the relativistic corrections to the scattering amplitudes are important. We should mention also the eventual presence of the off-shell effects which are very difficult to estimate.

4. $p\text{-}{}^4\text{He}$ backward scattering

In Ref. [3] we have discussed the $p\text{-}{}^4\text{He}$ data [1] at 298, 438 and 648 MeV incoming proton energy. Here we add our results for the differential cross section at 840 MeV or 6.0 GeV/c incoming α -particle momentum. They are presented in Fig. 10. At 840 MeV we observe a rather steep peak in the backward direction. Comparing the absolute magni-

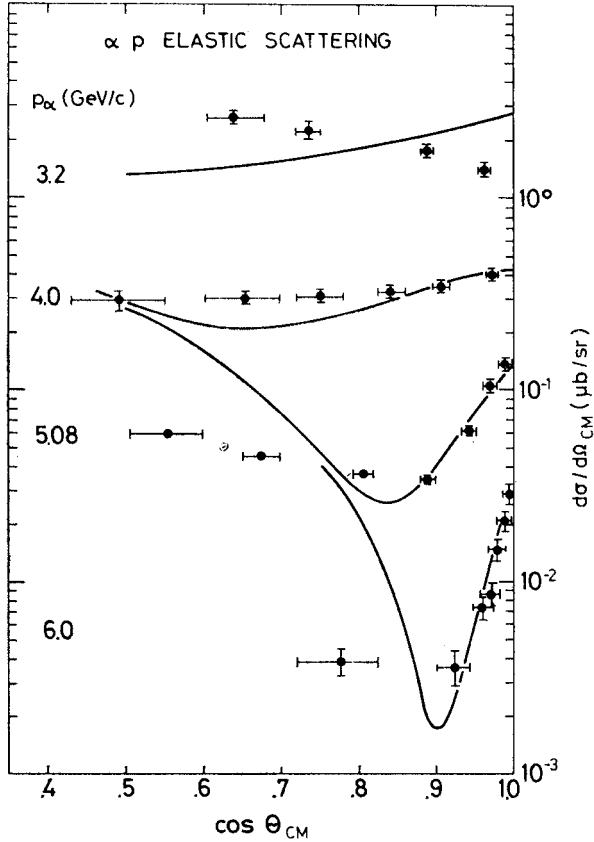


Fig. 10. Proton- ${}^4\text{He}$ elastic scattering at 298, 438, 648 and 840 MeV. Data are from Ref. [1]. Parameters at 840 MeV are: $\sigma_p = 48$ mb, $\alpha_p = 0.05$, $a_p = 4$ GeV $^{-2}$, $\text{Re } \varepsilon = -0.52$, $\alpha_t = -0.07$, $B = 0.52$ fm $^{-2}$, at lower energies — see Ref. [3]

tudes we notice that the cross section falls down quickly with the proton energy. The general features of the angular distributions are rather well described by the triton exchange model with the absorptive corrections perhaps except for the smallest energy. One should note that the momentum transfers at 300 MeV are close to the position of the zero of the proton-triton wave function and therefore the cross sections in this energy range are sensitive to different corrections which are needed in the present model. Especially at small energies the eikonal approximation may break down as well as the simple parametrization of the pp and pt scattering amplitudes.

5. Conclusions

The deuteron and triton-exchange models explain many features of the backward proton- ^3He or proton- ^4He elastic scattering differential cross sections. The cross sections calculated in the Born approximation are substantially changed by the absorption effects in the initial and final channels. These effects are calculated in the eikonal approximation. The general agreement is better for the p- ^4He case where the absorption effects produce the steep peaks in the backward direction. For the p- ^3He case the approximate equality of the 415 and 600 MeV differential cross sections is not reproduced by the model although the shape and the order of magnitude of the cross sections are well predicted. The possible reasons for this discrepancy are discussed in Section 3. It would be desirable to measure the proton-triton backward scattering cross section in order to test the predictions of the exchange model. For the proton-triton elastic scattering only the $I = 1$ two-neutron exchange contributes while for the p- ^3He case $I = 0$ and $I = 1$ exchanges are allowed. In addition the data on ^4He and ^3He electromagnetic form factors at higher momentum transfers would help us to understand better the internal structure of these nuclei.

We would like to thank Dr J. Thirion for the hospitality extended to us at CEN Saclay where a part of this work was done and to Professor N. Marty, Drs R. Beurtey, I. Brissaud, R. Frascaria, L. Goldzahl, J. Oostens and W. T. H. van Oers for many discussions of their experimental data.

REFERENCES

- [1] J. Berger et al., *Phys. Lett.* **63B**, 111 (1976).
- [2] R. Frascaria et al., *Phys. Lett.* **66B**, 329 (1977).
- [3] H. Leśniak et al., *Nucl. Phys.* **A267**, 503 (1976).
- [4] M. L. Goldberger, K. M. Watson, *Collision Theory*, Wiley, New York 1964, p. 153.
- [5] T. K. Lim, *Phys. Lett.* **43B**, 349 (1973).
- [6] J. S. McCarthy et al., *Phys. Rev. Lett.* **25**, 884 (1970).
- [7] T. Janssens et al., *Phys. Rev.* **142**, 922 (1966).
- [8] A. A. Vorobyov et al., *Phys. Lett.* **41B**, 639 (1972).
- [9] D. Aebischer et al., *Phys. Rev.* **D13**, 2478 (1976).
- [10] P. Söding, *Phys. Lett.* **8**, 285 (1964).
- [11] R. E. Hendrick, B. Lautrup, *Phys. Rev.* **D11**, 529 (1975).
- [12] D. V. Bugg et al., *Phys. Rev.* **146**, 980 (1966).

- [13] O. Benary, R. R. Price, G. Alexander, Lawrence Radiation Laboratory report UCRL-20000 NN (1970).
- [14] J. Bystricky, F. Lehar, Z. Janout, CEN Saclay report CEA-N-1547 /E/ (1972).
- [15] L. M. Dutton et al., *Nucl. Phys.* **B9**, 594 (1969).
- [16] A. V. Crewe et al., *Phys. Rev.* **114**, 1361 (1959).
- [17] E. T. Boschitz et al., *Phys. Rev.* **C6**, 457 (1972).
- [18] J. Fain et al., *Nucl. Phys.* **A262**, 413 (1976).
- [19] J. D. Seagrave, in *Three Body Problem in Nuclear and Particle Physics*, ed. J. S. C. Mc Kee and P. M. Rolph, North-Holland, Amsterdam-London 1970, p. 41.
- [20] V. I. Komarov et al., *Yad. Fiz.* **11**, 711 (1970).
- [21] F. Gibson, *Nucl. Phys.* **B2**, 501 (1967).
- [22] Y. E. Kim, A. Tubis, *Ann. Rev. Nucl. Sci.* **24**, 69 (1974).
- [23] G. W. Barry, *Phys. Rev.* **D7**, 1441 (1973).